ORIGINAL ARTICLE

Diaphragm Muscle Fiber Weakness and Ubiquitin–Proteasome Activation in Critically Ill Patients

Pleuni E. Hooijman[1], Albertus Beishuizen[2,3], Christian C. Witt[4], Monique C. de Waard[2], Armand R. J. Girbes[2], Angelique M. E. Spoelstra-de Man[2], Hans W. M. Niessen[5,6], Emmy Manders[1], Hieronymus W. H. van Hees[7], Charissa E. van den Brom[8], Vera Silderhuis[3], Michael W. Lawlor[9], Siegfried Labeit[10], Ger J. M. Stienen[1,11], Koen J. Hartemink[6,12], Marinus A. Paul[6], Leo M. A. Heunks[13], and Coen A. C. Ottenheijm[1,14]

[1]Department of Physiology, [2]Department of Intensive Care, [5]Department of Pathology, [6]Department of Cardiothoracic Surgery, and [8]Department of Anesthesiology, CaR-VU, VU University Medical Center, Amsterdam, the Netherlands; [3]Intensive Care and Medisch Spectrum Twente, Enschede, the Netherlands; [4]Department of Anesthesiology and Operative Intensive Care and [10]Department of Integrative Pathophysiology, Medical Faculty Mannheim, University of Heidelberg, Mannheim, Germany; [7]Department of Pulmonary Diseases and [13]Department of Intensive Care Medicine, Radboud University Medical Centre, Nijmegen, the Netherlands; [9]Division of Pediatric Pathology, Department of Pathology and Laboratory Medicine, Medical College of Wisconsin, Milwaukee, Wisconsin; [11]Faculty of Science, Department of Physics and Astronomy, VU University, Amsterdam, the Netherlands; [12]Department of Surgery, Netherlands Cancer Institute–Antoni van Leeuwenhoek Hospital, Amsterdam, the Netherlands; and [14]Department of Physiology, University of Arizona, Tucson, Arizona

Abstract

Rationale: The clinical significance of diaphragm weakness in critically ill patients is evident: it prolongs ventilator dependency, and increases morbidity and duration of hospital stay. To date, the nature of diaphragm weakness and its underlying pathophysiologic mechanisms are poorly understood.

Objectives: We hypothesized that diaphragm muscle fibers of mechanically ventilated critically ill patients display atrophy and contractile weakness, and that the ubiquitin–proteasome pathway is activated in the diaphragm.

Methods: We obtained diaphragm muscle biopsies from 22 critically ill patients who received mechanical ventilation before surgery and compared these with biopsies obtained from patients during thoracic surgery for resection of a suspected early lung malignancy (control subjects). In a proof-of-concept study in a muscle-specific ring finger protein-1 (MuRF-1) knockout mouse model, we evaluated the role of the ubiquitin–proteasome pathway in the development of contractile weakness during mechanical ventilation.

Measurements and Main Results: Both slow- and fast-twitch diaphragm muscle fibers of critically ill patients had approximately 25% smaller cross-sectional area, and had contractile force reduced by half or more. Markers of the ubiquitin–proteasome pathway were significantly up-regulated in the diaphragm of critically ill patients. Finally, MuRF-1 knockout mice were protected against the development of diaphragm contractile weakness during mechanical ventilation.

Conclusions: These findings show that diaphragm muscle fibers of critically ill patients display atrophy and severe contractile weakness, and in the diaphragm of critically ill patients the ubiquitin–proteasome pathway is activated. This study provides rationale for the development of treatment strategies that target the contractility of diaphragm fibers to facilitate weaning.

Keywords: single muscle fiber; diaphragm weakness; mechanical ventilation; weaning failure

(Received in original form December 12, 2014; accepted in final form February 23, 2015)

Supported by a VIDI grant from the Netherlands Foundation for Scientific Research (C.A.C.O.), NHLBI grant HL-121500 (C.A.C.O.), the National Institutes of Health (K08AR059750 and L40 AR057721; M.W.L.), and a grant from the German Research Foundation (DFG: WI 3278/2-2; C.C.W.).

Author Contributions: P.E.H., study coordination, literature search, figures, data collection and analysis, data interpretation, and writing. A.B., study design, patient inclusion, data interpretation, and writing. C.C.W., H.W.M.N., E.M., H.W.H.v.H., C.E.v.d.B., M.W.L., and S.L., data collection and analysis, data interpretation, and writing. M.C.d.W. and A.M.E.S.-d.M., patient inclusion, study coordination, and writing. A.R.J.G., study design and writing. V.S., patient inclusion and writing. G.J.M.S. and L.M.A.H., data interpretation and writing. K.J.H., obtaining biopsies, patient inclusion, data interpretation, and writing. M.A.P., study design, obtaining biopsies, patient inclusion, and writing. C.A.C.O., study coordination, literature search, study design, data interpretation, and writing.

Correspondence and requests for reprints should be addressed to Coen A. C. Ottenheijm, Ph.D., Department of Physiology, VU University Medical Center, 1081 BT Amsterdam, the Netherlands. E-mail: c.ottenheijm@vumc.nl

This article has an online supplement, which is accessible from this issue's table of contents at www.atsjournals.org

Am J Respir Crit Care Med Vol 191, Iss 10, pp 1126–1138, May 15, 2015

Originally Published in Press as DOI: 10.1164/rccm.201412-2214OC on March 11, 2015
Internet address: www.atsjournals.org

At a Glance Commentary

Scientific Knowledge on the Subject: The clinical significance of diaphragm weakness in critically ill patients is evident: it prolongs ventilator dependency and increases morbidity and duration of hospital stay. To date, the nature of diaphragm weakness and its underlying pathophysiologic mechanisms are poorly understood.

What This Study Adds to the Field: Our findings of atrophy, contractile weakness, and ubiquitin–proteasome pathway activation suggest that changes at the muscle fiber level may account for the *in vivo* diaphragm weakness observed in critically ill patients.

Patients with critical illness experience substantial skeletal muscle weakness and physical disability. This leads to functional impairment of survivors of the intensive care unit (ICU), an impairment that can last for years (1–3). In particular, weakness of the diaphragm (the main muscle of inspiration) is of major concern in critically ill patients: it prolongs ventilator dependency, increases morbidity and duration of hospital stay, and is associated with long-term functional limitations after hospital discharge (4–7).

Diaphragm weakness in mechanically ventilated critically ill patients has been established with noninvasive measurements; ultrasound revealed reduced motion and thinning of the diaphragm (8–10), and by magnetic stimulation of the phrenic nerves a reduced capacity to generate pressure was observed (11–14). The cellular changes that underlie diaphragm weakness in critically ill patients are unclear. For instance, changes in phrenic nerve function, in neuromuscular transmission, or in the contractility of individual muscle fibers all may explain the reduction in pressure generation by the diaphragm.

Critical illness–associated phenomena, such as mechanical ventilation (MV)–induced diaphragm inactivity (15–20), malnutrition (21), and inflammation (22), are associated with weakness of diaphragm fibers and activation of proteolytic pathways in animal models. Whether these findings translate to humans is unknown, although several studies (23–25), but not all (26), in brain-dead organ donors who received MV before organ harvest revealed atrophy and activation of the ubiquitin–proteasome pathway in diaphragm muscle fibers. Based on these observations, it was suggested that changes at the level of the individual diaphragm fibers play a critical role in the development of diaphragm weakness in critically ill patients. However, brain-dead organ donors do not exhibit the clinical features of critically ill patients; complete absence of neural activation of the diaphragm, metabolic stress, and brain ischemia differentiates them. Consequently, it is unknown whether these findings translate to critically ill patients. Establishing whether in critically ill patients the individual diaphragm muscle fibers exhibit contractile weakness is of utmost importance, because this provides rationale for treatment strategies that specifically improve the contractility of diaphragm fibers to facilitate weaning (27–29).

Therefore, in the present study we hypothesized that in the diaphragm of critically ill patients (1) muscle fibers display atrophy and contractile weakness, and (2) the ubiquitin–proteasome pathway is activated. To test these hypotheses, we obtained biopsies of the diaphragm of 22 critically ill patients who received MV before surgery, and compared these biopsies with those obtained from patients undergoing resection of an early lung malignancy (control subjects). We determined the size and the contractile strength of individual muscle fibers, which were type-identified. Additionally, we evaluated critical components of the ubiquitin–proteasome pathway, and performed proof-of-concept studies in muscle-specific ring finger protein-1 (MuRF-1) knockout (KO) mice to evaluate the role of this pathway in the development of contractile weakness during MV. Some of the present findings were published as pilot data in a letter (29).

Methods

For further details on the applied methods, *see* the online supplement.

Patients

Diaphragm and noninspiratory muscle biopsy specimens were obtained from mechanically ventilated critically ill patients (n = 22) and from patients undergoing resection of a suspected early lung malignancy (control subjects, n = 14). The biopsy protocol was approved by the institutional review board at VU University Medical Center, Amsterdam (#2010/69). Written informed consent was obtained from the patient or a legal representative.

Histology

Serial cryosections were cut from the biopsies and stained to study general structure, inflammatory infiltrates, and fiber cross-sectional area (CSA).

Contractility Experiments

For contractility experiments, the composition of solutions was as described previously (30–32) and the protocol was adapted from Ottenheijm and colleagues (33).

Protein Analyses

Myosin heavy chain isoform composition and concentration. Following the contractile experiments, myosin heavy chain (MyHC) isoform composition of the single fibers was identified by sodium dodecyl sulfate–polyacrylamide gel electrophoresis, as described previously with minor modifications (33).

Assay of ubiquitin ligases and ubiquitin-conjugated proteins. The levels of MuRF-1, muscle atrophy F-box (MAFbx), and ubiquitin–protein conjugates in muscle biopsies were examined by Western blotting.

Electron Microscopy

Electron microscopy was performed at the Electron Microscopy Core Facility at the Medical College of Wisconsin.

Animal Experiments

Wild-type and MuRF-1 KO mice were randomly split into two groups: one underwent MV for 6 hours (MV KO mice, n = 6; MV wild-type mice, n = 6) and the other group, not receiving MV, served as control (control KO mice, n = 8, control wild-type mice, n = 6). The contractile properties of intact diaphragm muscle bundles were measured as described previously (34).

Statistical Analysis

Because of the limited biopsy size not all parameters were determined in all biopsies

Table 1. Medical History and Reason for Admission of ICU Patients

No.	Age (*yr*)	Sex	Muscle	Relevant Past Medical History	Reason Admission to ICU	Surgery Where Biopsy Was Obtained	Septic	Died	BMI (kg/m^2)	APACHE II
1	48	F	LD	COPD GOLD I	Respiratory failure after VATS lobectomy	Rethoracotomy: lobectomy necrotic middle lobe	N	N	18	22
2	67	M	RA	Concentric left ventricle hypertrophy with decreased ejection fraction	Hemorrhagic shock due to retroperitoneal hematoma	Final closure of abdominal wound after relaparotomy	N	Y	28	38
3	67	F	RA	Rheumatoid arthritis, cerebrovascular accident	Septic shock due to intestinal perforation, small bowel resection	Relaparotomy: second look, drainage abdomen	Y	Y	22	18
4	53	M	LD	None	Thoracic endovascular aortic repair for type B dissection, hemorrhagic shock	Thoracotomy with surgical reevacuation hematothorax	N	N	30	29
5	47	F	RA	None	Severe trauma	Relaparotomy: removal of gauze, had emergency surgery previously for retroperitoneal hematoma and pericardial fenestration	N	N	22	28
6	67	F	RA	Hypertension, cigarette smoker, thyroid dysfunction	Gastroenteric ischemia, thrombosis of celiac trunk and AMS/ endovascular treatment	Relaparotomy for drainage abdominal abscess	Y	Y	23	28
7	26	F	RA	Thalassemia	Severe trauma	Relaparotomy: removal of gauze	N	N	25	44
8	66	M	RA	Hypertension	Abdominal sepsis due to appendicitis perforation	Laparotomy for removal of Bogota bag and drainage	Y	N	29	11
9	70	M	LD	None	Esophageal rupture, Boerhaave syndrome	Thoracotomy	N	N	22	27
10	51	M	RA	None	Severe trauma and traumatic shock	Relaparotomy for removal of gauze	N	N	29	30
11	46	F	RA	Asthma, cigarette smoker	In-hospital cardiac arrest due to hemorrhagic shock from abdominal origin	Relaparotomy for removal of gauze	N	Y	19	37
12	52	M	RA	None	Severe trauma	Relaparotomy for closing abdomen	Y	N	29	20
13	81	F	PM	Hypertension	Severe trauma	Thorax surgery reconstruction two ribs and inspection	N	Y	24	32
14	77	F	RA	Diabetes mellitus II	Cecal perforation with sepsis, acute kidney failure	Relaparotomy for removal of Bogota bag	Y	Y	28	21
15	71	M	RA	COPD GOLD I, colon carcinoma	Duodenal perforation with sepsis	Relaparotomy for cholecystectomy perforation gallbladder	Y	Y	20	19
16	77	F	RA	Spinal cord injury level L4-L5	Gastrointestinal perforation	Relaparotomy for removal of Bogota bag and drainage	Y	Y	23	22
17	74	M	RA	Hypertension, atrial fibrillation	Respiratory failure due to pneumonia, ICU stay complicated by bowel perforation	Relaparotomy for evacuation hematoma	Y	Y	25	19
18	83	M	RA	Hypertension, polyposis, SAH, rectum carcinoma	Abdominal sepsis, Hartmann procedure	Relaparotomy for removal of Bogota bag, hemicolectomy	Y	Y	24	35
19	68	M	RA	COPD GOLD II, radiotherapy for prostate carcinoma	Aortic dissection, hematothorax after Bentall procedure, rib fracture after cardiopulmonary resuscitation	Thoracotomy for fixation of rib fractures	N	N	24	16
20	68	F	—	Hypertension, noninsulin-dependent diabetes, cerebral infarction	Respiratory failure due to upper airway obstruction complicated by type II myocardial infarction	Coronary artery bypass graft surgery and hemistrumectomy	N	Y	27	18
21	69	F	RA	Hypertension, smoker, aortic valve replacement	Progressive heart failure after surgery aortic valve replacement, perforation of transverse colon	Relaparotomy for drainage ascites	N	Y	34	16
22	22	F	RA	None	Severe trauma	Relaparotomy for closing abdomen	N	N	20	31

Definition of abbreviations: AMS = superior mesenteric artery; APACHE = Acute Physiology and Chronic Health Evaluation II score at first 24 h of admission to ICU; BMI = body mass index; COPD = chronic obstructive pulmonary disease; GOLD = Global Initiative for Chronic Obstructive Lung Disease; ICU = intensive care unit; LD = latissimus dorsi muscle; No. = number; PM = pectoralis major muscle; RA = rectus abdominis muscle; SAH = subarachnoid hemorrhage; VATS = video-assisted thoracic surgery.

(*see* Table E2 in the online supplement). Outcome of continuous measurements that were normally distributed are presented as the mean ± SEM and were compared using group *t* tests. Outcome of continuous measurements that were not normally distributed are presented as the median and the interquartile range, and were compared using Mann-Whitney tests.

Results

Patients

The demographic and clinical characteristics of all patients are shown in Tables 1–3.

Diaphragm Fiber CSA and Inflammatory Cells

Figure 1A shows representative examples of diaphragm cryosections stained with hematoxylin and eosin and Figure 1B with antibodies specific for fast MyHC. Quantification of CSA showed that diaphragm muscle fibers are atrophied in critically ill patients: slow-twitch fibers were 22% smaller (control subjects vs. critically ill, 3,013 ± 845 vs. 2,335 ± 728 μm^2; $P = 0.02$) and fast-twitch fibers were 30% smaller (control subjects vs. critically ill, 2,899 ± 820 vs. 1,998 ± 580 μm^2; $P = 0.001$) (Figure 1C). The fraction of slow- and fast-twitch fibers did not differ between control subjects and critically ill patients (data not shown). Figure 1D shows examples of stainings with inflammatory cell markers. The number of neutrophilic granulocytes and macrophages were significantly higher in diaphragm cryosections of critically ill patients, but the number of lymphocytes did not differ between groups (Figure 1E).

Diaphragm Muscle Fiber Contractility

Most fibers expressed exclusively MyHC I (referred to as slow-twitch) or MyHC 2A (fast-twitch). In line with previous work on human diaphragm (30, 33, 35), approximately 6% of the total number of fibers in both patient groups expressed MyHC 2X, and the data from these fibers were pooled with those from fibers expressing MyHC 2A. Fibers that coexpressed MyHC isoforms were classified according to the dominant isoform. Note that our findings do not indicate that the percentage of fibers that coexpressed MyHC isoforms increased in critically ill patients.

Figure E1 in the online supplement shows a typical force measurement. The maximal absolute force was significantly lower in muscle fibers of critically ill patients: control subjects versus critically ill, slow-twitch fibers, respectively, 0.42 (0.36–0.48) versus 0.19 (0.13–0.25) mN, $P < 0.0001$; and fast-twitch fibers, respectively, 0.52 (0.39–0.67) versus 0.23 (0.16–0.40) mN, $P = 0.005$ (Figure 2A). Thus, individual diaphragm fibers of critically ill patients show severe contractile weakness.

By normalizing absolute force to the CSA of the muscle fiber (i.e., tension), we determined whether the reduction of force was proportional to the reduction of the CSA. Maximal tension was significantly lower in slow-twitch fibers of critically ill patients: control subjects versus critically ill, respectively, 125 ± 18 versus 94 ± 31 mN/mm^2, $P = 0.004$. Fast-twitch fibers showed a trend toward a reduction in maximal tension, control subjects versus critically ill, respectively, 156 ± 25 versus 132 ± 41 mN/mm^2, $P = 0.06$ (Figure 2B).

The active force generated by sarcomeres in permeabilized single muscle

Table 2. Specification of Duration and Settings of Mechanical Ventilation

No.	PC (*h*)	PS (*h*)	NR or O_2 Mask* (*h*)	Total MV (*h*)	Respiratory Rate (min^{-1})	$F_{I_{O_2}}$	Peak Pressure ($cm\ H_2O$)	$Pa_{O_2}/F_{I_{O_2}}$ ($mm\ Hg$)	PEEP ($cm\ H_2O$)
1	29	1	0	30	27 ± 1.4	1 ± 0	31 ± 1	55 ± 12	9 ± 1.4
2	200	403	4	607	25 ± 8.1	0.5 ± 0.1	24 ± 3	174 ± 59	9 ± 1.7
3	28	0	0	28	29 ± 1.4	0.4 ± 0	21 ± 1	245 ± 16	5 ± 0
4	254	58	6	318	30 ± 7.4	0.7 ± 0.2	35 ± 4	134 ± 46	16 ± 3.3
5	34	0	4	38	47 ± 20	0.6 ± 0.2	32 ± 8	216 ± 11	12 ± 1.1
6	45	292	0	337	23 ± 3.9	0.4 ± 0.0	26 ± 3	219 ± 16	6 ± 0.6
7	132	81	7	220	35 ± 9.3	1 ± 0	44 ± 1	135 ± 73	17 ± 7.1
8	2	25	21*	48	14 ± 2.4	0.4 ± 0.0	11 ± 1	236 ± 7	4 ± 0.0
9	8	5	1	14	37 ± 12.7	0.8 ± 0.2	26 ± 2	150 ± 2	12 ± 0
10	82	0	4	86	26 ± 5.8	0.1 ± 0.0	18 ± 5	219 ± 21	14 ± 0
11	60	0	2	62	18 ± 1.5	0.4 ± 0.0	19 ± 1	237 ± 16	8 ± 0.8
12	147	161	0	308	20 ± 5.8	0.4 ± 0.0	18 ± 5	268 ± 0	7 ± 2.6
13	44	0	0	44	20 ± 2.9	0.4 ± 0.0	26 ± 3	245 ± 4	7 ± 0.1
14	22	0	0	22	23 ± 2.1	0.4 ± 0.0	26 ± 1	192 ± 22	10 ± 0.0
15	14	8	0	22	22 ± 2.6	0.5 ± 0.0	18 ± 1	193 ± 11	4 ± 0.0
16	16	32	0	48	11 ± 1.1	0.4 ± 0.0	17 ± 2	244 ± 1	4 ± 0.0
17	170	216	48*	434	16 ± 5.1	0.4 ± 0.2	24 ± 5	223 ± 60	9 ± 2.7
18	48	0	0	48	22 ± 1.4	0.5 ± 0.0	20 ± 1	193 ± 8	10 ± 0
19	17	205	278*	500	50 ± 9.5	0.4 ± 0.1	28 ± 4	165 ± 38	8 ± 2.4
20	6	81	3	90	44 ± 11.1	0.4 ± 0.1	21 ± 6	149 ± 28	8 ± 0.8
21	116	112	9	237	21 ± 2.5	0.4 ± 0.1	27 ± 5	222 ± 25	8 ± 0.5
22	106	90	6	202	46 ± 9.4	0.4 ± 0.1	38 ± 17	218 ± 69	8 ± 0.8

Definition of abbreviations: No. = number; NR = nonregistered (e.g., during transport of the patient, or during surgery); O_2 mask = hours ventilated via oxygen mask; PC = pressure control; PEEP = positive end-expiratory pressure; PS = pressure support; Total MV = sum of hours on mechanical ventilation from moment of intubation until biopsy (*see* Table E2 for details).
Data are totals or mean ± SD. Ventilatory settings are averaged from moment of intubation until biopsy.
*Patients on O_2 mask.

Table 3. Medical History of Control Patients

No.	Sex	Noninsp Muscle	Age (*yr*)	Removed Tumor	Relevant Medical History	MV (*h*)	BMI (kg/m^2)	FEV_1	FEV_1 %pred	FEV_1/FVC %pred	FVC	FVC %pred	VC %pred
1*	M	SA	52	pT3N0M0	Cigarette smoker, diabetes mellitus II, hypertension	1.5	25	2.3	68	0.69	3.3	76	NA
2*	M	SA	22	pT1bN0M0	Cigarette smoker	2.0	23	4.7	103	0.71	6.7	121	NA
3	M	LD	66	pT2aN1M0	Cigarette smoker, hypertension, prostate cancer, COPD	2.0	24	2.7	82	0.66	4.2	NA	97
4	F	LD	58	pT1aN0M0	None	2.0	28	2.9	104	0.77	3.7	NA	116
5	M	LD	60	pT1aN1M0	Cigarette smoker, s/p right upper lobectomy for T1 N0 M0 lung cancer, pulmonary tuberculosis s/p successful drug therapy	1.5	24	3.8	97	0.67	5.6	113	108
6	M	LD	56	pT4N2M0	Cigarette smoker, COPD	2.0	21	3.1	78	0.52	5.9	118	NA
7	M	LD	70	pT1bN1M0	Cigarette smoker, s/p basal cell cancer skin	1.5	30	2.9	89	0.69	4.3	NA	96
8	F	LD	60	pT2aN0R0	Hypertension	0.75	26	2.9	127	0.86	3.4	NA	120
9	F	LD	59	Cyst	Cigarette smoker	0.75	28	2.0	79	0.75	NA	NA	NA
10	F	LD	64	pT1bN0M0	COPD	1.25	26	1.9	76	0.62	3.1	NA	NA
11	F	LD	59	Adenocarcinoma CT2BN2M1A	Cigarette smoker, cholecystectomy, COPD	0.75	21	2.1	76	0.64	3.2	101	94
12	M	LD	52	pT2N0M0	Cigarette smoker	1.00	23	3.2	81	0.73	4.7	110	NA
13	M	LD	64	Bronchiectasis and inflammation, benign	Hypertension, 6 yr ago MI with PCI of LAD artery, diabetes mellitus II	1.00	31	2.41	92	0.72	3.3	86	86
14	F	LD	74	Inflammation with central necrosis, benign	Bronchiectasis and allergic bronchopulmonary aspergillosis	2.50	21	1.79	82	0.67	2.7	103	NA

Definition of abbreviations: %pred = percentage of predicted value; BMI = body mass index; COPD = chronic obstructive pulmonary disease; LAD = left anterior descending artery; LD = latissimus dorsi; MI = myocardial infarct; MV = mechanical ventilation; NA = not available; No. = number; Noninsp Muscle = muscle biopsy from noninspiratory muscle; PCI = percutaneous coronary intervention; SA = serratus anterior; s/p = status post.
*Lung function of these patients was measured after surgery where biopsy was obtained.

fibers is largely determined by (*1*) the fraction of strongly bound cross-bridges, (*2*) the number of available cross-bridges, and (*3*) the force per cross-bridge (36, 37). A reduction in maximal tension should be accompanied by a change in one or more of these three determinants.

The rate constant for force redevelopment (ktr) provides information on the attachment and detachment rate of the cross-bridges during activation and reflects the fraction of strongly bound cross-bridges. Ktr did not differ between control subjects and critically ill patients: slow-twitch fibers, respectively, 5.5 (5.0–6.2) versus 4.8 (4.4–6.3) s^{-1}, $P = 0.18$; fast-twitch fibers, respectively, 12.9 ± 2.6 versus 10.9 ± 3.6 s^{-1}, $P = 0.12$ (Figure 3A).

The number of attached cross-bridges during activation is estimated by measuring the active stiffness (Figure 3B). Active stiffness, normalized to fiber size, was significantly reduced, control subjects versus critically ill, respectively, 75 ± 11 versus 50 ± 17 $mN/mm^2/\Delta L$, $P = 0.002$; and fast-twitch fibers, 62 ± 13 versus 46 ± 10 $mN/mm^2/\Delta L$, $P = 0.003$ (Figure 3C).

In a situation in which all myofibrils in the individual muscle fiber are intact, the force generated per cross-bridge is reflected in the tension/stiffness ratio. The tension/stiffness ratio was not significantly different between control subjects and critically ill patients, respectively: 1.9 ± 0.2 versus 2.2 ± 0.6, $P = 0.16$ in slow-twitch fibers; and 2.9 ± 0.6 versus 3.1 ± 0.6, $P = 0.53$ in fast-twitch fibers (Figure 3D). Thus, together, our findings indicate that the reduced tension of diaphragm muscle fibers of critically ill patients is caused by a reduction in the number of attached cross-bridges during activation.

To determine whether the reduced number of attached cross-bridges is caused by a reduction in the concentration of contractile protein, fibers were demounted following the contractility experiments, and the abundance of MyHC was analyzed with sodium dodecyl sulfate–gel electrophoresis using known standards of MyHC (Figure 4A). The MyHC concentration did not differ between control subjects and

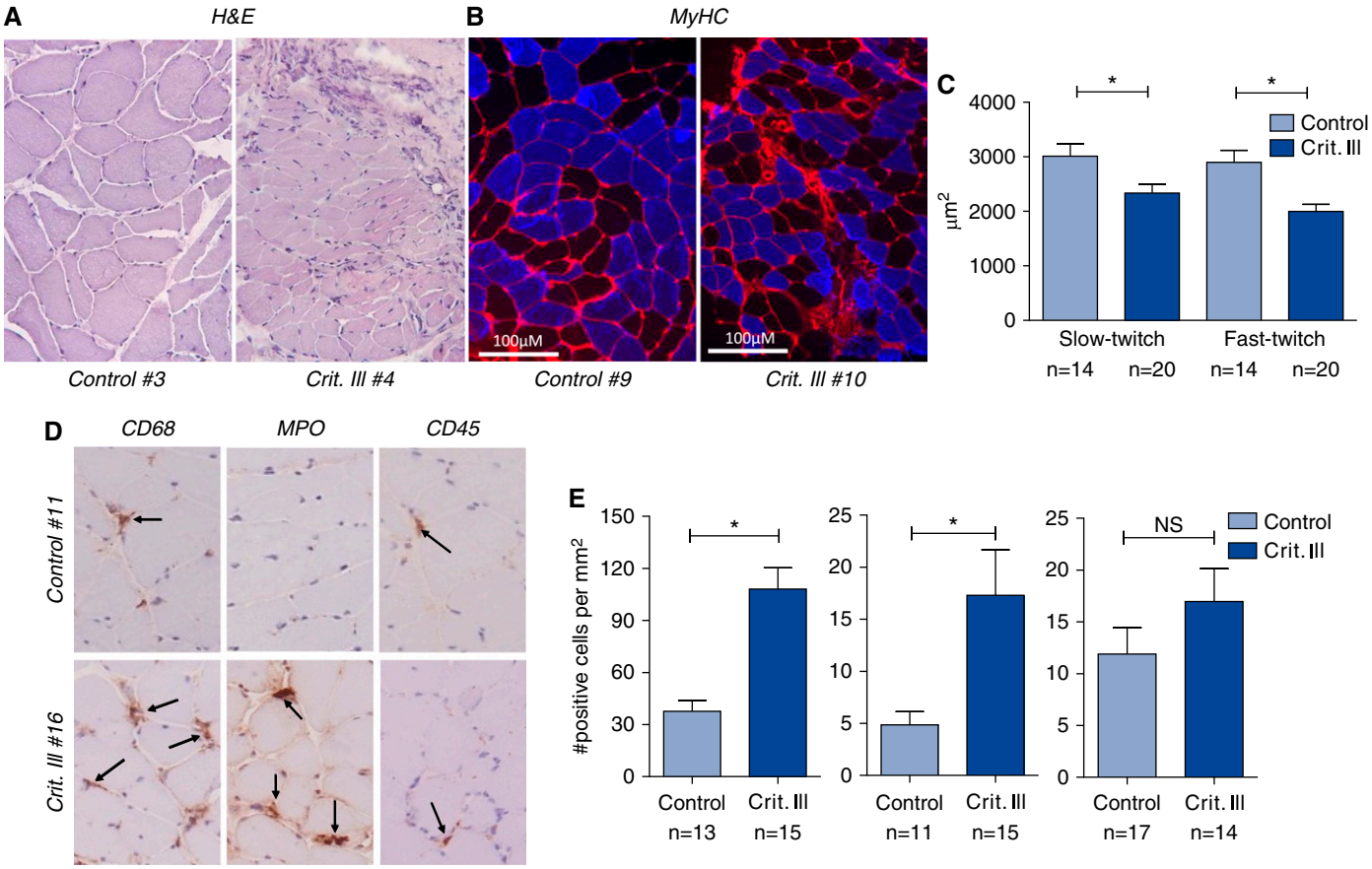

Figure 1. Atrophy of diaphragm fibers in critically ill patients. (*A*) Representative examples of hematoxylin and eosin (H&E) staining. (*B*) Immunohistochemically stained cross-sections of diaphragm muscle fiber biopsies. *Red*: wheat germ agglutinin indicating membranes. *Blue*: MY32 antibody specific for fast-twitch fibers. (*C*) Diaphragm fiber cross-sectional area (μm^2) was significantly smaller in slow- and fast-twitch fibers of critically ill patients, indicating atrophy. (*D*) Representative examples of staining for macrophages (CD68), neutrophil granulocytes (myeloperoxidase [MPO]), and lymphocytes (CD45). (*E*) In critically ill patients, the number of macrophages and neutrophil granulocytes was significantly higher compared with control subjects. MyHC = myosin heavy chain; NS = not significant. *$P < 0.05$. *Arrows* indicate inflammatory cells.

critically ill patients: slow-twitch fibers, respectively, 64 ± 21 versus 80 ± 22 μg/ml, $P = 0.09$; fast-twitch fibers, respectively, 66 ± 16 versus 69 ± 21 μg/ml, $P = 0.67$ (Figure 4B). Thus, whereas the number of attached cross-bridges was reduced in fibers of critically ill patients (Figure 3C), the MyHC concentration was not. This suggests the presence of myofibrillar damage in these diaphragm fibers.

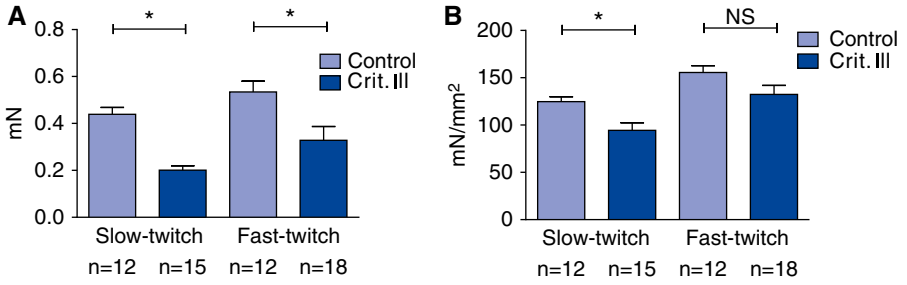

Figure 2. Contractile weakness of individual diaphragm fibers in critically ill patients. (*A*) The maximal absolute force generation of both slow- and fast-twitch diaphragm muscle fibers of critically ill patients was significantly lower compared with control patients. (*B*) Maximal tension, which is the absolute maximal force normalized to fiber cross-sectional area, was significantly lower in slow-twitch fibers of critically ill patients compared with control fibers, and fast-twitch fibers showed a trend toward a lower maximal tension. NS = not significant. *$P < 0.05$.

To verify whether diaphragm fibers of critically ill patients indeed contained damaged contractile material, we investigated the ultrastructure by electron microscopy in one critically ill patient and in one control subject. Figure 5 shows that in the control subject myofibrils were well aligned with well-defined Z-disks, I-bands, and A-bands. However, diaphragm fibers of the critically ill patient contained areas of myofibrillar disarray. Overall, our findings reveal that individual diaphragm fibers of critically ill patients are severely weakened, both by atrophy and by dysfunction of the remaining contractile proteins.

The Ubiquitin–Proteasome Pathway

Figure 6A shows that the ubiquitin ligases MuRF-1 and MAFbx, two important

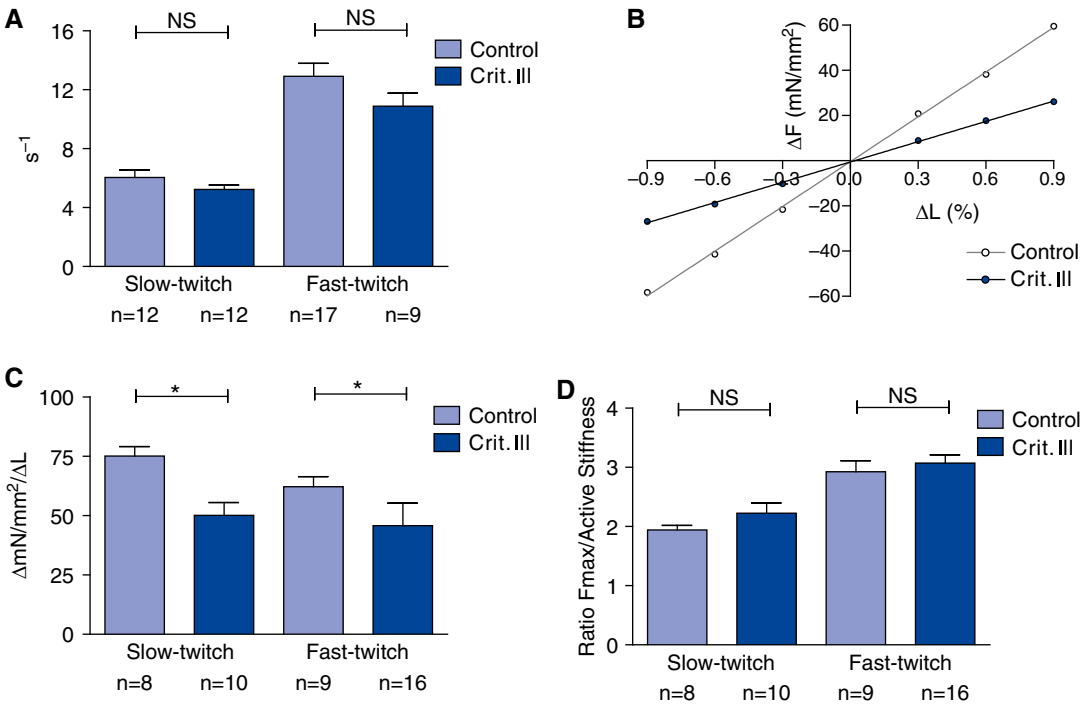

Figure 3. Cross-bridge cycling kinetics. (*A*) The rate constant of force redevelopment did not differ between control and critically ill patients in both fiber types, which suggests there is no reduction in the fraction of strongly bound cross-bridges. (*B*) Amplitude of the force response (normalized to cross-sectional area) during fiber shortening and lengthening; the slope of this line is the normalized active stiffness (shown are representative single diaphragm fibers of critically ill patient 1 and control patient 1). (*C*) Normalized active stiffness was significantly lower in slow- and fast-twitch fibers of critically ill patients. (*D*) The ratio of maximal tension to normalized active stiffness, which is a measure of the force generated per cross-bridge, did not differ between critically ill and control patients. NS = not significant. *$P < 0.05$.

markers of atrophy, are present in diaphragm muscle homogenates of control patients, indicating that these ligases are part of the common protein turnover system. Using quantitative Western blotting, we observed that diaphragm muscle homogenates of critically ill patients had twofold higher MuRF-1 levels (control vs. critically ill, 1.0 [0.4–1.1] vs. 2.1 [1.5–4.0]; $P = 0.001$) (Figure 6B); and more than threefold higher MAFbx levels (control subjects vs. critically ill patients, respectively, 0.6 [0.3–1.1] vs. 2.2 [1.0–3.7]; $P = 0.002$) (Figure 6C).

Figure 6D shows a representative example of Western blotting with antiubiquitin antibodies. In diaphragm fibers of critically ill patients, the level of protein ubiquitination was more than fourfold higher compared with control subjects: control versus critically ill, respectively, 1.0 (0.5–2.6) versus 4.4 (3.7–5.6), $P = 0.011$ (Figure 6E).

Role of MuRF-1 in the Development of Diaphragm Weakness during MV

The common denominator in the critically ill patients is that they are exposed to MV. Animal studies have indicated that MV induces activation of the ubiquitin–proteasome pathway, and that MuRF-1 specifically targets sarcomeric proteins. Therefore, we mechanically ventilated (for 6 h) MuRF-1 wild-type and MuRF-1 KO mice and compared the contractile strength of intact diaphragm muscle bundles with nonventilated (control) mice. In wild-type mice, MV induced a 30% reduction in the maximal tetanic force of intact diaphragm bundles; control subjects versus MV, respectively, 241 ± 12 versus 165 ± 36 mN/mm^2 ($P = 0.03$). However, in MuRF-1 KO mice no effect of MV on diaphragm strength was observed: MV versus control, respectively, 231 ± 31 versus 241 ± 32 mN/mm^2 ($P = 0.586$) (Figure 7A). Furthermore, there was a rightward shift of the force-stimulation frequency relation in diaphragm bundles of MV wild-type mice compared with control wild-type mice (Figure 7B). Such shift was not observed after MV in MuRF-1 KO mice ($P = 0.76$) (Figure 7C). Thus, in mice, MuRF-1 is critical to the development of diaphragm weakness during MV.

Noninspiratory Muscles in Critically Ill Patients

To determine whether the changes in diaphragm fibers were part of a generalized muscle weakness, we also studied biopsies of noninspiratory muscles of the same patients. The CSA of slow-twitch fibers of noninspiratory muscles in control and critically ill patients was, respectively, 2,878 (2,256–3,704) versus 2,388 (1,801–3,606) μm^2 ($P = 0.41$); and fast-twitch fibers, 3,311 (1,918–4,759) versus 2,757 (1,287–3,983) μm^2 ($P = 0.27$) (Figure 8).

Ubiquitin ligase levels and protein ubiquitination were up-regulated in noninspiratory muscle homogenates of critically ill patients compared with control subjects (Figure 9); MuRF-1, control subjects versus critically ill, respectively, 3.9 (1.1–6.5) versus 29.0 (16.2–49.0), $P = 0.005$; MAFbx, control subjects versus critically ill, respectively, 1.0 (0.4–2.2) versus 9.5 (2.6–14.1), $P = 0.020$. Levels of protein ubiquitination also significantly differed between control and critically ill patients, respectively, 0.7 ± 0.1 versus 2.8 ± 0.6

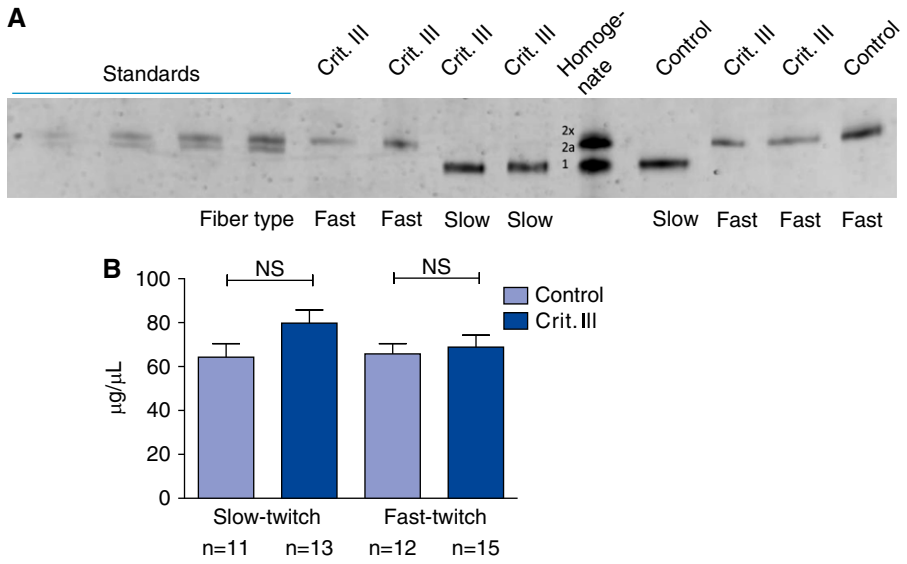

Figure 4. Myosin heavy chain (MyHC) concentration is preserved in diaphragm fibers of critically ill patients. (*A*) Example of sodium dodecyl sulfate–gel electrophoresis with known amounts of rabbit MyHC (M-1636 Sigma) to determine the amount of MyHC per fiber volume. (*B*) MyHC concentration of slow- and fast-twitch fibers did not differ between control and critically ill patients. NS = not significant.

($P = 0.005$). Thus, the ubiquitin–proteasome pathway was activated in noninspiratory muscles of critically ill patients, but no significant difference in fiber CSA was observed.

Discussion

This study shows that both slow- and fast-twitch diaphragm muscle fibers of mechanically ventilated critically ill patients display atrophy and severe contractile weakness. These findings were associated with marked activation of the ubiquitin–proteasome pathway in the diaphragm of critically ill patients.

Contractile Weakness of Individual Diaphragm Fibers in Critically Ill Patients

Investigation of diaphragm muscle biopsies is indispensable to elucidate the nature of diaphragm weakness in critically ill patients. The biopsies provide ways to study muscle fiber structure and size, and importantly they enable the determination of the contractile properties of individual diaphragm fibers. Because diaphragm biopsies are obtained from the belly of the muscle, the fiber ends are disrupted, which precludes electrical activation of the fibers. Therefore we permeabilized the fibers, and subsequently activated them with exogenous calcium. We observed a greater than 50% reduction in the force-generating capacity of diaphragm fibers of critically ill patients, a reduction that was observed in both slow- and fast-twitch muscle fibers. This weakness was caused by fiber atrophy, and by dysfunction of the sarcomeric proteins. Considering the magnitude of contractile weakness, we propose that these changes at the diaphragm muscle fiber level largely account for the 30–50% reduction in *in vivo* diaphragm strength in critically ill patients, as measured by bilateral phrenic nerve stimulation (11, 13, 14, 38–40).

Our results from biopsies cannot exclude that mechanisms residing outside the diaphragm fibers, such as phrenic nerve dysfunction, contribute to diaphragm weakness in critically ill patients. Only little information is available on phrenic nerve function in critically ill patients. Demoule and colleagues (41) reported prolonged phrenic nerve conduction time in some critically ill patients. However, most patients they studied experienced prolonged weaning failure, whereas the study populations in which *in vivo* diaphragm strength was determined did not represent such severe clinical status. Data from MV animal models indicated reduction of diaphragm strength *in vivo* (17) despite normal phrenic nerve function. In these animals, reduction of *in vitro* strength of diaphragm strips was of the same magnitude as the strength reduction observed *in vivo*, indicating that changes at diaphragm fiber level were the main cause for the loss of contractility. Thus, our findings indicate that abnormalities in the contractility of individual diaphragm fibers contribute to the diaphragm weakness in critically ill patients.

Activation of the Ubiquitin–Proteasome Pathway in the Diaphragm

Activation of the ubiquitin–proteasome pathway may, at least partially, explain the development of diaphragm weakness in critically ill patients. In this pathway, proteins are labeled with ubiquitin molecules, which target them for degradation by the proteasome (31, 32). The conjugation of ubiquitin to proteins is under control of ubiquitin ligases. MuRF-1 and MAFbx are striated muscle-specific ubiquitin ligases, and both are considered important markers of atrophy (42). Protein levels of MuRF-1 and MAFbx were markedly elevated in diaphragm tissue of critically ill patients. As expected, the increased ubiquitin ligase activity resulted in increased levels of ubiquitinated proteins. The contribution of other proteolytic mechanisms to diaphragm weakening in critically ill patients cannot be excluded. For instance, protein kinase B (AKT) regulates transcription of MAFbx and MuRF-1 (43) during atrophy, but simultaneously regulates the autophagy pathway (25, 44–46), and before the ubiquitin–proteasome pathway can be effective, myofibrils have to be dismantled by caspases and/or calpains (47). Also, activation of proteolytic pathways occurs simultaneously with deactivation of anabolic pathways to limit the energy expenditure for the production of novel proteins (48). Accordingly, in a comparable group of critically ill patients, a decrease in MyHC mRNA expression was found in vastus lateralis and rectus femoris muscle biopsies (38, 39), indicating decreased protein synthesis rates. Future studies should address whether such anabolic pathways also are affected in the diaphragm of critically ill patients.

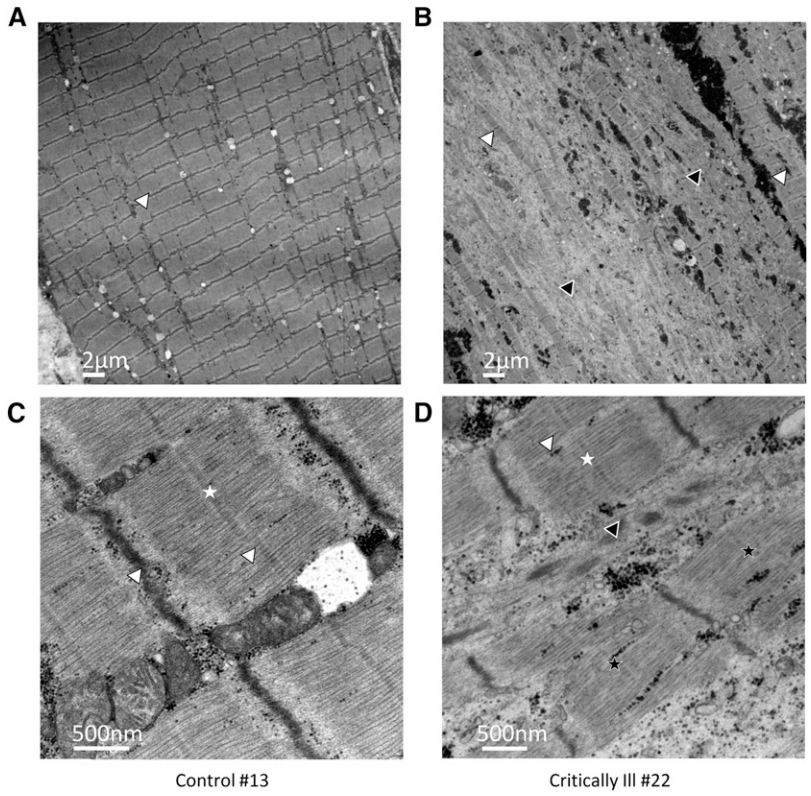

Figure 5. Ultrastructural damage in diaphragm fibers of critically ill patients. Electron microscopy images of longitudinal sections of diaphragm muscle fibers. (*A* and *C*) Control patient; (*B* and *D*) critically ill patient. The diaphragm samples of the control patient show intact structure with mostly well-aligned myofibrils. The diaphragm sample of the critically ill patient shows myofibrils that are disarranged (*white arrowheads* and *black arrowheads* indicate, respectively, well-arranged and disarranged myofibrils and z-disks; *white stars* and *black stars* indicate, respectively, well-arranged and disarranged M-lines).

Activation of the ubiquitin–proteasome pathway and the development of diaphragm muscle fiber weakness may be caused by several phenomena that are associated with critical illness, including malnutrition, lung injury, inflammation, and inactivity. The heterogeneity of the patient population studied here warrants caution when speculating regarding the main phenomena at play. A common denominator in the critically ill patients was their exposure to MV. Therefore, we evaluated the specific role of MuRF-1 in diaphragm weakening during MV, because MuRF-1 is known to target myosin (49), and myosin is essential for proper contractile function of skeletal muscle fibers. Earlier studies showed that diaphragm weakness develops during controlled MV of mice (20), but we show that weakness does not develop in the absence of MuRF-1 (Figure 7). This suggests that MuRF-1 is important for the development of diaphragm weakness during MV. Whether MV contributed to MuRF-1 activation and diaphragm weakness in our patients cannot be established, because ventilatory settings differed greatly per patient and as a result their level of diaphragm activity as well. In animals, low levels of diaphragm activity are known to mitigate the detrimental effects of MV on diaphragm strength (50).

To gain more insight into whether systemic factors contributed to the changes observed in the diaphragm, we also studied biopsies of noninspiratory muscles from the same patients. Our rationale was that if systemic factors are at play, a generalized muscle weakness ought to develop. We observed activation of proteolytic machinery in noninspiratory muscles while fiber atrophy had not (yet) developed. Previous work revealed that during atrophic stimuli E3 ligase levels first increase but subsequently decrease although fiber atrophy continues (51). In line with these observations, Wollersheim and colleagues (39) revealed up-regulation of E3 ligases in quadriceps muscle 5 days after ICU admission, a time point at which atrophy had not developed yet, whereas after 15 days the E3-ligase levels were back to control levels but fiber atrophy had started to develop.

Our findings may be consistent with these studies, if one assumes that in the critically ill patients the atrophic stimulus was stronger in the diaphragm than in the noninspiratory muscles: diaphragmatic E3 ligase levels were already on the descending limb of their relation with time (and atrophy was evident), whereas in the noninspiratory muscles the E3 ligase levels were still on the ascending limb of this relation and fiber atrophy had not yet developed. Note that this assumption is based on recent work in animal models showing that, compared with peripheral muscles, the diaphragm is more susceptible to systemic inflammation (52), and that the interactive effects of MV and systemic inflammation exacerbate diaphragm weakness (53). Thus, a combination of MV and systemic phenomena may accelerate weakening of the diaphragm. However, to firmly establish whether changes in the diaphragm precede those in nonrespiratory muscles requires serial biopsies of both muscle types within critically ill patients. Clearly, the acquisition of serial diaphragm biopsies poses a considerable challenge.

Study Limitations

Several limitations of our study should be noted. First, the group of critically ill patients included was rather heterogeneous in admission diagnosis, duration of MV, past medical history, and so forth. This, in combination with the sample size, precludes the identification of meaningful associations between clinical entities and diaphragm atrophy or weakness. However, this is the typical mix of patients admitted to a medical–surgical ICU, and therefore the data of this study are relevant for typical ICU patients.

Second, 4 of the 14 control patients had mild obstructive lung disease, a condition that has been associated with diaphragm dysfunction (33). Consequently, the magnitude of diaphragm fiber weakness in

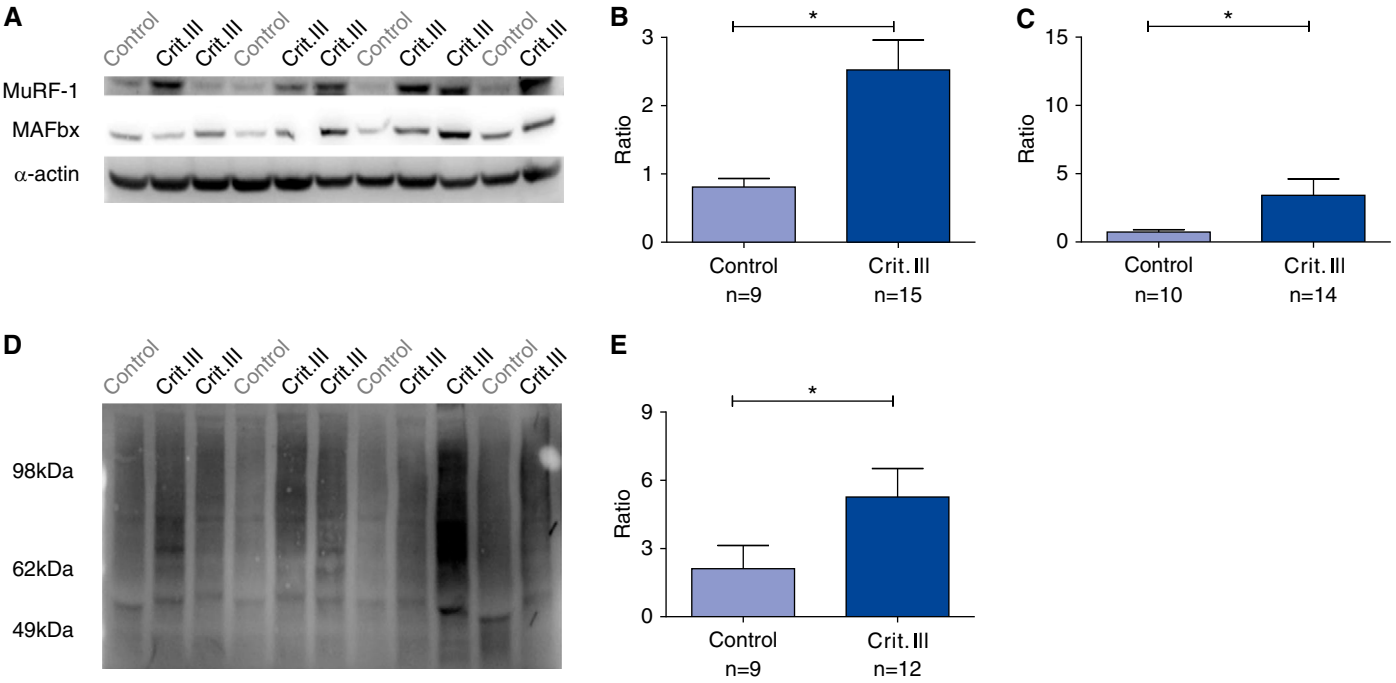

Figure 6. Increased activation of the ubiquitin–proteasome pathway in diaphragm fibers of critically ill patients. (*A*) Example of Western blot; each lane represents diaphragm muscle homogenates of control and critically ill patients with antibodies for the ubiquitin ligases muscle-specific ring finger protein-1 (MuRF-1) (*top*), muscle atrophy F-box (MAFbx) (*middle*), and α-actin (*bottom*, loading control). In critically ill patients compared with control subjects, there was a significant increase in protein levels of MuRF-1 (twofold, *B*) and MAFbx (more than threefold, *C*) relative to α-actin (note that each sample was normalized to a reference control sample that was run on each gel). (*D*) Example of a Western blot with an antiubiquitin antibody to detect ubiquitinated proteins; each lane represents a diaphragm muscle homogenate of a control or a critically ill patient. (*E*) The relative level of ubiquitinated proteins was more than fourfold higher in critically ill patients compared with control subjects. *$P < 0.05$.

critically ill patients might be underestimated.

Third, the noninspiratory muscle biopsies were mostly obtained from rectus abdominis muscle in the critically ill patients (Table 1), and from latissimus dorsi muscle in the control patients (Table 3). Caution is warranted when comparing different muscles. However, a post-mortem study in healthy humans (39) showed that the rectus abdominis muscle has a slightly smaller fiber diameter than latissimus dorsi muscle. Thus, it is highly unlikely that differences between muscle types masked the presence of fiber atrophy in the noninspiratory muscles of the critically ill patients. Furthermore, reports suggest that latissimus dorsi and pectoralis major muscles may aid in deep inspiration, which warrants caution when extrapolating the results from these muscles to "true" noninspiratory muscles.

Clinical Implications

In recent years, the focus on developing therapies to combat diaphragm weakening and weaning failure in critically ill patients

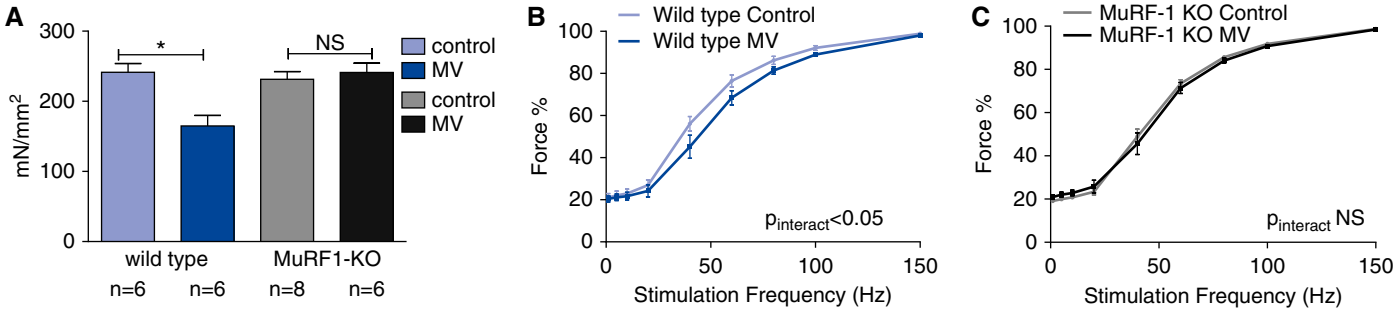

Figure 7. Intact diaphragm muscle strength in muscle-specific ring finger protein-1 (MuRF-1) knockout (KO) mice. Intact diaphragm muscle strips were isolated from wild-type and MuRF-1 KO mice. (*A*) Maximal tetanic force was significantly lower in wild-type mice that received mechanical ventilation (MV) compared with wild-type mice that did not receive MV (control subjects). Diaphragm muscle strength of MV MuRF-1 KO mice did not differ from control MuRF-1 KO mice. (*B*) Compared with the control group, in MV wild-type mice a rightward shift of the force–stimulation frequency relation was present; (*C*) this rightward shift was not present in MV MuRF-1 KO mice. NS = not significant. *$P < 0.05$.

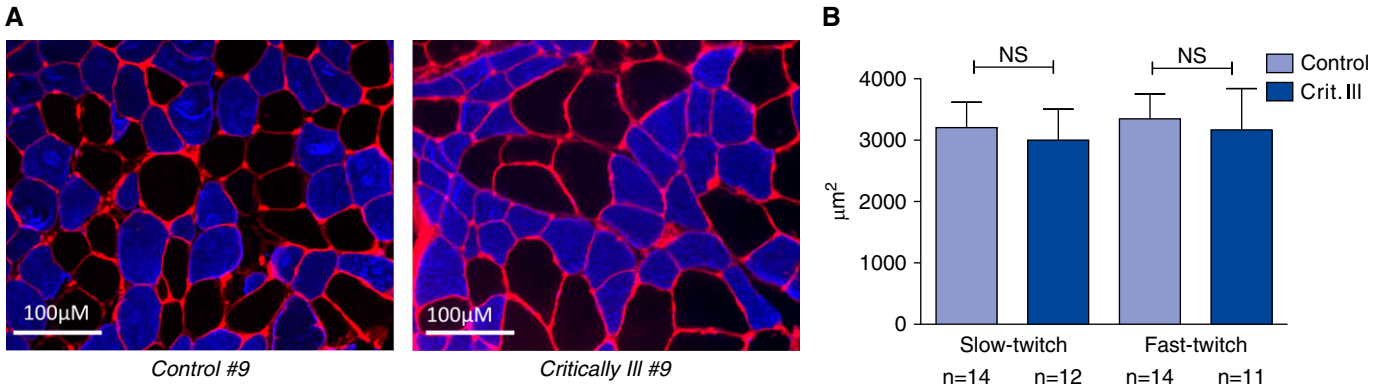

Figure 8. Noninspiratory muscles of critically ill patients do not exhibit fiber atrophy. (*A*) Representative examples of immunohistochemically stained cross-sections of biopsies of latissimus dorsi muscle. *Red*: wheat germ agglutinin indicating membranes. *Blue*: MY32 antibody specific for fast-twitch fibers. (*B*) Fiber cross-sectional area (μm^2) of noninspiratory muscles did not differ between control and critically ill patients. NS = not significant.

has expanded. The present findings indicate that targeting the contractility of sarcomeres might be a powerful therapeutic approach. Indeed, levosimendan, a drug that sensitizes the sarcomeres for calcium, improves fiber strength (27) and neuromechanical efficiency (28) in the human diaphragm. In a pilot study on critically ill patients we recently showed that the fast skeletal troponin activator CK-2066260, an analog of tirasemtiv, which is tested in clinical trials for amyotrophic lateral sclerosis, significantly augments the *ex vivo* contractile strength of diaphragm muscle fibers (29). Future studies should test the efficacy of these drugs in improving success of weaning in critically ill patients.

An alternative approach might be to inhibit proteasome activity. Proteasome inhibitors have been successfully used to block atrophy in various animal models

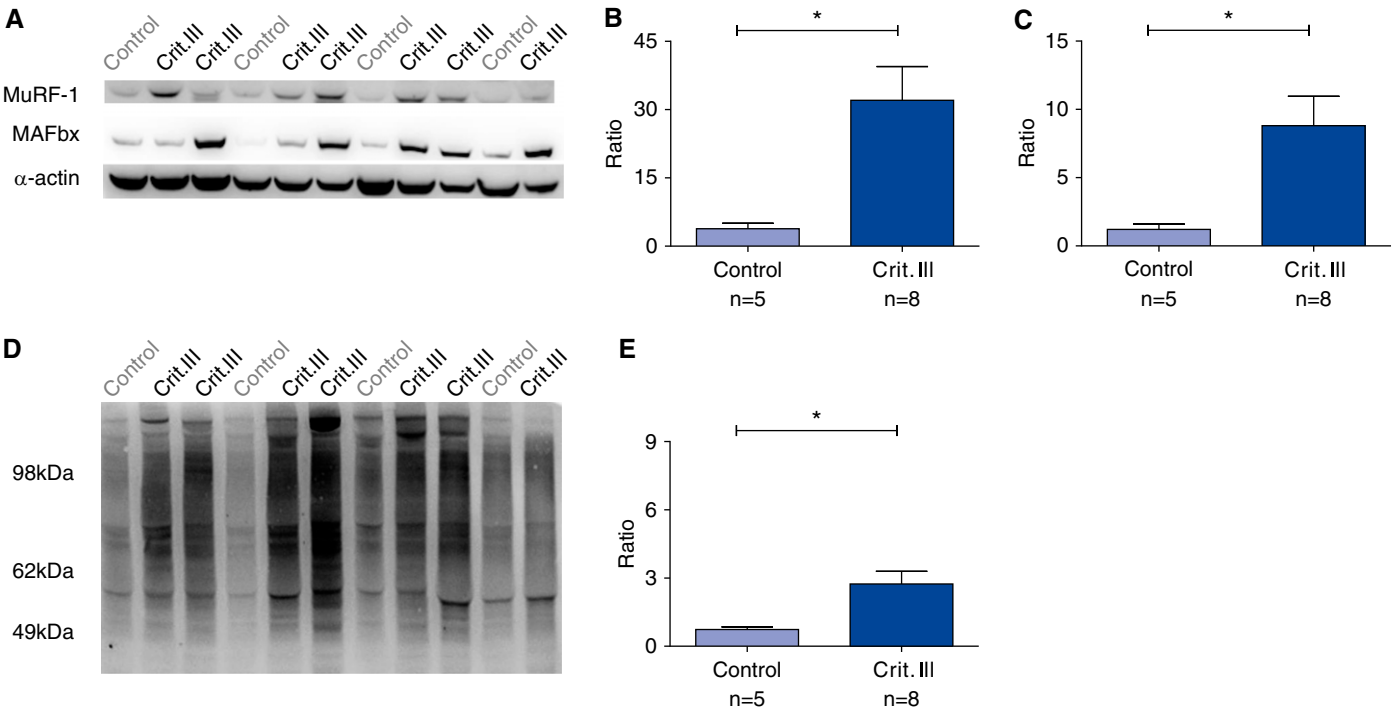

Figure 9. Increased activation of the ubiquitin–proteasome pathway in noninspiratory muscles of critically ill patients. (*A*) Example of a Western blot. Each lane represents diaphragm muscle homogenates of control and critically ill patients with antibodies for the ubiquitin ligases muscle-specific ring finger protein-1 (MuRF-1) (*top*), muscle atrophy F-box (MAFbx) (*middle*), and α-actin (*bottom*, loading control). In critically ill patients compared with control subjects, there was a significant increase in protein levels of MuRF-1 (more than sevenfold, *B*) and MAFbx (more than ninefold, *C*) relative to α-actin (note that each sample was normalized to a reference control sample that was run on each gel). (*D*) Example of a Western blot with an antiubiquitin antibody to detect ubiquitinated proteins; each lane represents a diaphragm muscle homogenate of a control or a critically ill patient. (*E*) The relative level of ubiquitinated proteins was more than fourfold higher in critically ill patients compared with control subjects. $^*P < 0.05$.

(54–58). However, prolonged inhibition of general protein degradation is likely to have a major impact on protein quality control, and may ultimately be detrimental for several cell types. A more elegant approach is to target ubiquitin ligases, because they are tissue-specific and their activity is the rate-limiting step in the ubiquitin–proteasome pathway (42). Earlier studies showed that MuRF-1 KO mice are resistant to denervation-induced muscle atrophy (51) and that knockdown of MAFbx spares muscle mass in fasted animals (59). Our finding of preserved diaphragm strength in MuRF-1–deficient mice during MV further strengthens the idea that slowing down of proteolysis by targeting ubiquitin-ligases might be a successful therapeutic approach to facilitate weaning. To date, inhibitors of ubiquitin ligases, such as MuRF-1, are not available.

Conclusions

Our findings are the first to show contractile weakness and activation of the ubiquitin–proteasome pathway in diaphragm fibers of critically ill patients. The severity of the weakness suggests that changes at the diaphragm fiber level can largely account for the *in vivo* diaphragm weakness in the critically ill. Accordingly, clinical interventions aimed at improving diaphragm fiber contractility should be considered when designing future weaning trials. ■

Author disclosures are available with the text of this article at www.atsjournals.org.

References

1. Batt J, Dos Santos CC, Herridge MS. Muscle injury during critical illness. *JAMA* 2013;310:1569–1570.
2. Schweickert WD, Hall J. ICU-acquired weakness. *Chest* 2007;131: 1541–1549.
3. Herridge MS, Tansey CM, Matté A, Tomlinson G, Diaz-Granados N, Cooper A, Guest CB, Mazer CD, Mehta S, Stewart TE, *et al*.; Canadian Critical Care Trials Group. Functional disability 5 years after acute respiratory distress syndrome. *N Engl J Med* 2011;364:1293–1304.
4. De Jonghe B, Bastuji-Garin S, Sharshar T, Outin H, Brochard L. Does ICU-acquired paresis lengthen weaning from mechanical ventilation? *Intensive Care Med* 2004;30:1117–1121.
5. Boles J-M, Bion J, Connors A, Herridge M, Marsh B, Melot C, Pearl R, Silverman H, Stanchina M, Vieillard-Baron A, *et al*. Weaning from mechanical ventilation. *Eur Respir J* 2007;29:1033–1056.
6. Esteban A, Anzueto A, Frutos F, Alía I, Brochard L, Stewart TE, Benito S, Epstein SK, Apezteguía C, Nightingale P, *et al*.; Mechanical Ventilation International Study Group. Characteristics and outcomes in adult patients receiving mechanical ventilation: a 28-day international study. *JAMA* 2002;287:345–355.
7. Laghi F, Tobin MJ. Disorders of the respiratory muscles. *Am J Respir Crit Care Med* 2003;168:10–48.
8. Kim WY, Suh HJ, Hong S-B, Koh Y, Lim C-M. Diaphragm dysfunction assessed by ultrasonography: influence on weaning from mechanical ventilation. *Crit Care Med* 2011;39:2627–2630.
9. DiNino E, Gartman EJ, Sethi JM, McCool FD. Diaphragm ultrasound as a predictor of successful extubation from mechanical ventilation. *Thorax* 2014;69:423–427.
10. Grosu HB, Lee YI, Lee J, Eden E, Eikermann M, Rose KM. Diaphragm muscle thinning in patients who are mechanically ventilated. *Chest* 2012;142:1455–1460.
11. Demoule A, Jung B, Prodanovic H, Molinari N, Chanques G, Coirault C, Matecki S, Duguet A, Similowski T, Jaber S. Diaphragm dysfunction on admission to the intensive care unit. Prevalence, risk factors, and prognostic impact-a prospective study. *Am J Respir Crit Care Med* 2013;188:213–219.
12. Man WD-C, Moxham J, Polkey MI. Magnetic stimulation for the measurement of respiratory and skeletal muscle function. *Eur Respir J* 2004;24:846–860.
13. Jaber S, Petrof BJ, Jung B, Chanques G, Berthet J-P, Rabuel C, Bouyabrine H, Courouble P, Koechlin-Ramonatxo C, Sebbane M, *et al*. Rapidly progressive diaphragmatic weakness and injury during mechanical ventilation in humans. *Am J Respir Crit Care Med* 2011; 183:364–371.
14. Hermans G, Agten A, Testelmans D, Decramer M, Gayan-Ramirez G. Increased duration of mechanical ventilation is associated with decreased diaphragmatic force: a prospective observational study. *Crit Care* 2010;14:R127.
15. Shanely RA, Zergeroglu MA, Lennon SL, Sugiura T, Yimlamai T, Enns D, Belcastro A, Powers SK. Mechanical ventilation-induced diaphragmatic atrophy is associated with oxidative injury and increased proteolytic activity. *Am J Respir Crit Care Med* 2002;166:1369–1374.
16. Le Bourdelles G, Viires N, Boczkowski J, Seta N, Pavlovic D, Aubier M. Effects of mechanical ventilation on diaphragmatic contractile properties in rats. *Am J Respir Crit Care Med* 1994;149:1539–1544.
17. Sassoon CSH, Caiozzo VJ, Manka A, Sieck GC. Altered diaphragm contractile properties with controlled mechanical ventilation. *J Appl Physiol (1985)* 2002;92:2585–2595.
18. Bernard N, Matecki S, Py G, Lopez S, Mercier J, Capdevila X. Effects of prolonged mechanical ventilation on respiratory muscle ultrastructure and mitochondrial respiration in rabbits. *Intensive Care Med* 2003;29:111–118.
19. Radell PJ, Remahl S, Nichols DG, Eriksson LI. Effects of prolonged mechanical ventilation and inactivity on piglet diaphragm function. *Intensive Care Med* 2002;28:358–364.
20. Mrozek S, Jung B, Petrof BJ, Pauly M, Roberge S, Lacampagne A, Cassan C, Thireau J, Molinari N, Futier E, *et al*. Rapid onset of specific diaphragm weakness in a healthy murine model of ventilator-induced diaphragmatic dysfunction. *Anesthesiology* 2012;117:560–567.
21. Lewis MI, Sieck GC, Fournier M, Belman MJ. Effect of nutritional deprivation on diaphragm contractility and muscle fiber size. *J Appl Physiol (1985)* 1986;60:596–603.
22. Reid MB, Lännergren J, Westerblad H. Respiratory and limb muscle weakness induced by tumor necrosis factor-alpha: involvement of muscle myofilaments. *Am J Respir Crit Care Med* 2002;166:479–484.
23. Levine S, Biswas C, Dierov J, Barsotti R, Shrager JB, Nguyen T, Sonnad S, Kucharchzuk JC, Kaiser LR, Singhal S, *et al*. Increased proteolysis, myosin depletion, and atrophic AKT-FOXO signaling in human diaphragm disuse. *Am J Respir Crit Care Med* 2011;183:483–490.
24. Levine S, Nguyen T, Taylor N, Friscia ME, Budak MT, Rothenberg P, Zhu J, Sachdeva R, Sonnad S, Kaiser LR, *et al*. Rapid disuse atrophy of diaphragm fibers in mechanically ventilated humans. *N Engl J Med* 2008;358:1327–1335.
25. Hussain SN, Mofarrahi M, Sigala I, Kim HC, Vassilakopoulos T, Maltais F, Bellenis I, Chaturvedi R, Gottfried SB, Metrakos P, *et al*. Mechanical ventilation-induced diaphragm disuse in humans triggers autophagy. *Am J Respir Crit Care Med* 2010;182:1377–1386.
26. Hooijman PE, Paul MA, Stienen GJM, Beishuizen A, Van Hees HWH, Singhal S, Bashir M, Budak MT, Morgen J, Barsotti RJ, *et al*. Unaffected contractility of diaphragm muscle fibers in humans on mechanical ventilation. *Am J Physiol Lung Cell Mol Physiol* 2014; 307:L460–L470.
27. van Hees HWH, Dekhuijzen PNR, Heunks LMA. Levosimendan enhances force generation of diaphragm muscle from patients with chronic obstructive pulmonary disease. *Am J Respir Crit Care Med* 2009;179:41–47.
28. Doorduin J, Sinderby CA, Beck J, Stegeman DF, van Hees HW, van der Hoeven JG, Heunks LM. The calcium sensitizer levosimendan improves human diaphragm function. *Am J Respir Crit Care Med* 2012;185:90–95.
29. Hooijman PE, Beishuizen A, de Waard MC, de Man FS, Vermeijden JW, Steenvoorde P, Bouwman RA, Lommen W, van Hees HW, Heunks LM, *et al*. Diaphragm fiber strength is reduced in critically ill patients and restored by a troponin activator. *Am J Respir Crit Care Med* 2014;189:863–865.

30. Welvaart WN, Paul MA, Stienen GJ, van Hees HW, Loer SA, Bouwman R, Niessen H, de Man FS, Witt CC, Granzier H, *et al*. Selective diaphragm muscle weakness after contractile inactivity during thoracic surgery. *Ann Surg* 2011;254:1044–1049.
31. Ottenheijm CAC, Lawlor MW, Stienen GJM, Granzier H, Beggs AH. Changes in cross-bridge cycling underlie muscle weakness in patients with tropomyosin 3-based myopathy. *Hum Mol Genet* 2011; 20:2015–2025.
32. Ottenheijm CAC, Witt CC, Stienen GJ, Labeit S, Beggs AH, Granzier H. Thin filament length dysregulation contributes to muscle weakness in nemaline myopathy patients with nebulin deficiency. *Hum Mol Genet* 2009;18:2359–2369.
33. Ottenheijm CAC, Heunks LMA, Sieck GC, Zhan W-Z, Jansen SM, Degens H, de Boo T, Dekhuijzen PNR. Diaphragm dysfunction in chronic obstructive pulmonary disease. *Am J Respir Crit Care Med* 2005;172:200–205.
34. de Man FS, van Hees HWH, Handoko ML, Niessen HW, Schalij I, Humbert M, Dorfmüller P, Mercier O, Bogaard H-J, Postmus PE, *et al*. Diaphragm muscle fiber weakness in pulmonary hypertension. *Am J Respir Crit Care Med* 2011;183:1411–1418.
35. Ottenheijm CAC, Heunks LMA, Hafmans T, van der Ven PFM, Benoist C, Zhou H, Labeit S, Granzier HL, Dekhuijzen PNR. Titin and diaphragm dysfunction in chronic obstructive pulmonary disease. *Am J Respir Crit Care Med* 2006;173:527–534.
36. Brenner B. Effect of Ca2+ on cross-bridge turnover kinetics in skinned single rabbit psoas fibers: implications for regulation of muscle contraction. *Proc Natl Acad Sci USA* 1988;85:3265–3269.
37. Geiger PC, Cody MJ, Macken RL, Sieck GC, Paige C. Maximum specific force depends on myosin heavy chain content in rat diaphragm muscle fibers. *J Appl Physiol (1985)* 2000;89:695–703.
38. Puthucheary Z, Rawal J, McPhail M, Connolly B, Ratnayake G, Chan P, Hopkinson NS, Padhke R, Dew T, Sidhu PS, *et al*.Acute skeletal muscle wasting in critical illness. *JAMA* 2013;310:1591–1600.
39. Wollersheim T, Woehlecke J, Krebs M, Hamati J, Lodka D, Luther-Schroeder A, Langhans C, Haas K, Radtke T, Kleber C, *et al*. Dynamics of myosin degradation in intensive care unit-acquired weakness during severe critical illness. *Intensive Care Med* 2014;40: 528–538.
40. Powers SK, Kavazis AN, Levine S. Prolonged mechanical ventilation alters diaphragmatic structure and function. *Crit Care Med* 2009;37 (10 Suppl):S347–S353.
41. Demoule A, Morelot-Panzini C, Prodanovic H, Cracco C, Mayaux J, Duguet A, Similowski T. Identification of prolonged phrenic nerve conduction time in the ICU: magnetic versus electrical stimulation. *Intensive Care Med* 2011;37:1962–1968.
42. McKinnell IW, Rudnicki MA. Molecular mechanisms of muscle atrophy. *Cell* 2004;119:907–910.
43. Sandri M, Sandri C, Gilbert A, Skurk C, Calabria E, Picard A, Walsh K, Schiaffino S, Lecker SH, Goldberg AL. Foxo transcription factors induce the atrophy-related ubiquitin ligase atrogin-1 and cause skeletal muscle atrophy. *Cell* 2004;117:399–412.
44. Powers SK, Kavazis AN, McClung JM. Oxidative stress and disuse muscle atrophy. *J Appl Physiol (1985)* 2007;102:2389–2397.
45. Sandri M. Protein breakdown in muscle wasting: role of autophagy-lysosome and ubiquitin-proteasome. *Int J Biochem Cell Biol* 2013; 45:2121–2129.
46. Whidden MA, Smuder AJ, Wu M, Hudson MB, Nelson WB, Powers SK. Oxidative stress is required for mechanical ventilation-induced protease activation in the diaphragm. *J Appl Physiol (1985)* 2010; 108:1376–1382.
47. Du J, Wang X, Miereles C, Bailey JL, Debigare R, Zheng B, Price SR, Mitch WE. Activation of caspase-3 is an initial step triggering accelerated muscle proteolysis in catabolic conditions. *J Clin Invest* 2004;113:115–123.
48. Bonaldo P, Sandri M. Cellular and molecular mechanisms of muscle atrophy. *Dis Model Mech* 2013;6:25–39.
49. Clarke BA, Drujan D, Willis MS, Murphy LO, Corpina RA, Burova E, Rakhilin SV, Stitt TN, Patterson C, Latres E, *et al*. The E3 Ligase MuRF1 degrades myosin heavy chain protein in dexamethasone-treated skeletal muscle. *Cell Metab* 2007;6:376–385.
50. Sassoon CSH, Zhu E, Caiozzo VJ. Assist-control mechanical ventilation attenuates ventilator-induced diaphragmatic dysfunction. *Am J Respir Crit Care Med* 2004;170:626–632.
51. Bodine SC, Latres E, Baumhueter S, Lai VK-M, Nunez L, Clarke BA, Poueymirou WT, Panaro FJ, Na E, Dharmarajan K, *et al*. Identification of ubiquitin ligases required for skeletal muscle atrophy. *Science* 2001;294:1704–1708.
52. Li X, Moody MR, Engel D, Walker S, Clubb FJ Jr, Sivasubramanian N, Mann DL, Reid MB. Cardiac-specific overexpression of tumor necrosis factor-alpha causes oxidative stress and contractile dysfunction in mouse diaphragm. *Circulation* 2000;102:1690–1696.
53. Maes K, Stamiris A, Thomas D, Cielen N, Smuder A, Powers SK, Leite FS, Hermans G, Decramer M, Hussain SN, *et al*. Effects of controlled mechanical ventilation on sepsis-induced diaphragm dysfunction in rats. *Crit Care Med* 2014;42:e772–e782.
54. Caron AZ, Haroun S, Leblanc E, Trensz F, Guindi C, Amrani A, Grenier G. The proteasome inhibitor MG132 reduces immobilization-induced skeletal muscle atrophy in mice. *BMC Musculoskelet Disord* 2011; 12:185.
55. Jamart C, Raymackers J-M, Li An G, Deldicque L, Francaux M. Prevention of muscle disuse atrophy by MG132 proteasome inhibitor. *Muscle Nerve* 2011;43:708–716.
56. Supinski GS, Vanags J, Callahan LA. Effect of proteasome inhibitors on endotoxin-induced diaphragm dysfunction. *Am J Physiol Lung Cell Mol Physiol* 2009;296:L994–L1001.
57. Agten A, Maes K, Thomas D, Cielen N, Van Hees HWH, Dekhuijzen RPN, Decramer M, Gayan-Ramirez G. Bortezomib partially protects the rat diaphragm from ventilator-induced diaphragm dysfunction. *Crit Care Med* 2012;40:2449–2455.
58. van Hees H, Ottenheijm C, Ennen L, Linkels M, Dekhuijzen R, Heunks L. Proteasome inhibition improves diaphragm function in an animal model for COPD. *Am J Physiol Lung Cell Mol Physiol* 2011;301: L110–L116.
59. Cong H, Sun L, Liu C, Tien P. Inhibition of atrogin-1/MAFbx expression by adenovirus-delivered small hairpin RNAs attenuates muscle atrophy in fasting mice. *Hum Gene Ther* 2011;22:313–324.